Transfer functions of geophones and accelerometers and their effects on frequency content and wavelets

Michael S. Hons and Robert R. Stewart

ABSTRACT

Transfer functions for geophone and accelerometer transducers are derived. The mechanical deflection within the sensor and how that deflection is transformed into an electrical signal are both important in the derivation of transfer functions. For both transducers the output to the digitizer is the double time derivative of the ground displacement. Due to interactions of the mechanical system and the transducer, a geophone transducer reduces amplitude and adds phase lag to low frequencies. Wavelets calculated from the amplitude and phase spectra of the transducer transfer functions are shown. Next an input zero-phase wavelet is examined to find the differences resulting from its transformation by the transducers. Accelerometer transducers are found to produce negligible changes to the waveform, and the ground motion can be recovered through a double integration.

INTRODUCTION

The greatest opportunity for more interpretable seismic data provided by Micro Electro-Mechanical Systems (MEMS) based accelerometers is likely in their potential to record low frequencies in the acceleration domain without rolloff. Traditional geophones suffer significant reduction in recorded velocity-domain amplitudes below their natural frequency. MEMS accelerometers can record to fractions of 1 Hz without any relative reduction in acceleration amplitudes (Maxwell, 2001).

We explore the MEMS response in comparison to traditional geophones in two ways: derivation and modeling of the transfer functions, and convolution of an input wavelet with those transfer functions. Six transfer functions are derived and modeled: three each for a geophone transducer and a MEMS transducer. Each is only valid over the range of frequencies where the assumptions in the derivation hold true. Their transfer effects on an input wavelet are modeled.

THEORY

The Telecom Glossary 2K (2001), defines a transfer function as the relationship between the input and the output of a system, in terms of the transfer characteristics. Mathematically, it is given by

$$\frac{B}{A} = H \,, \qquad (1)$$

where B is the output, A is the input and H is the transfer function. When the transfer function operates on the input, the output is obtained. Laboratory testing of seismic sensors involves defining the input and precisely measuring the output to obtain the transfer function. The purpose here is modeling of the transfer function itself by varying the transfer characteristics, so that the relationship between any input and the corresponding output from the sensor system can be graphically inspected.

The simplest way to represent the response of a sensor is to focus on the transducer. The internal workings of a seismic sensor are discussed in more detail in Appendix A. The input to a transducer is the displacement of the proof mass relative to the sensor case. The output from a transducer is voltage. The magnitude of the output depends on how the transducer converts the proof mass displacement into voltage and the sensitivity of the instrument. Sensitivity will not be included in these equations, so the output from the transducer will be considered to be 'unscaled', or the actual voltage divided by sensitivity. So each of the transfer functions to be derived here are of the same form as equation (1), where B is the unscaled voltage produced by the transducer, A is the displacement of the proof mass relative to the case (A=x) and H is the transfer function, sometimes called the frequency response.

The transfer function of the transducer can be considered as a transfer function of the sensor under conditions where the displacement of the proof mass relative to the case (A) is approximately equal to the ground motion (u) in some domain (either displacement, velocity or acceleration). This results in the input to the transducer being directly related to the ground motion. All transfer functions will have the form B in terms of x divided by A (or x) in terms of u.

When the ratio of the measured frequencies to the natural frequency is small, then the displacement of the proof mass relative to the sensor case is nearly proportional to acceleration of the ground. So when $\omega \ll \omega_0$ it will be considered that the transducer responds to ground acceleration, or

$$A = \frac{\partial^2 u}{\partial t^2} . \qquad (2)$$

When the ratio is large, then the displacement of the proof mass relative to the sensor case is nearly proportional to the ground displacement. When $\omega \gg \omega_0$ then it will be considered that the transducer responds to ground displacement, or

$$A = u . \qquad (3)$$

When the ratio is neither small nor large (around 1) then the displacement of the proof mass relative to the case is nearly proportional to the velocity of the ground motion. When $\omega \cong \omega_0$ it will be considered that the transducer responds to ground velocity, or

$$A = \frac{\partial u}{\partial t} . \qquad (4)$$

How the displacement of the proof mass relative to the case is transformed into an electrical signal is an inherent property of the transducer. Accelerometers generally use a capacitive transducer to measure change in displacement, and it is the displacement of the proof mass relative to the case that is transformed into a voltage. In the case of a capacitive transducer we write

$$B = A = x\,, \tag{5}$$

where B is the unscaled voltage. Geophones use a coil around a magnet, which, through Faraday's Law of magnetic induction, responds only to the velocity of the proof mass. Thus it is the velocity of the proof mass relative to the case that is transformed into a voltage. In the case of an inductive transducer we write

$$B = \frac{\partial A}{\partial t} = \frac{\partial x}{\partial t}\,. \tag{6}$$

There is no commonly used transducer that responds only to acceleration.

A full derivation of the damped, forced simple harmonic motion equation can be found in Appendix A. This equation can be expressed as

$$\frac{\partial^2 x}{\partial t^2} + 2\lambda\omega_0 \frac{\partial x}{\partial t} + \omega_0^2 x = -\frac{\partial^2 u}{\partial t^2}\,, \tag{7}$$

where x is the displacement of the proof mass relative to the frame, u is the ground motion, λ is the damping ratio and ω_0 is the natural frequency (see Figure A1).

A simple way to solve the partial differential equation in (7) is by taking the Fourier Transform, which allows us to substitute $j\omega$ for d/dt. The simplest solution is for the displacement of the proof mass relative to the case (x) in terms of the displacement of the case (u). In the frequency domain

$$-\omega^2 X + 2j\lambda\omega_0\omega X + \omega_0^2 X = \omega^2 U\,, \tag{8}$$

which gives

$$\frac{X}{U} = \frac{\omega^2}{-\omega^2 + 2j\lambda\omega_0\omega + \omega_0^2}\,, \tag{9}$$

and is often expressed in engineering texts (Meirovitch, 1975) as

$$X = U\left(\frac{\omega}{\omega_0}\right)^2 H(\omega)\,, \tag{10}$$

where

$$H(\omega) = \frac{\dfrac{1}{\omega_0^2}}{-\dfrac{\omega^2}{\omega_0^2} + \dfrac{2j\lambda\omega}{\omega_0} + 1}\,. \tag{11}$$

An important distinction is that this equation is exact for all proof mass displacements relative to the case (x) in terms of any case displacement (y). However, this equation is only a transfer function for a transducer when it represents the transducer output divided by the input. This is true if the displacement between the proof mass and the case is directly proportional to the case displacement, and if the displacement between the proof mass and the case is directly transformed into a voltage. So the two conditions for this equation to be a transfer function are $\omega >> \omega_0$ and use of a capacitive transducer.

As mentioned above, the domain of the transducer is a fixed parameter of the sensor. So the left hand side of the following equations will be identical for all equations relating to one sensor. The right hand side can be expressed three different ways, depending on the ratio of the measured frequencies to the natural frequency. For a geophone, the following solutions are found:

$$j\omega \frac{\partial X}{\partial t} + 2\lambda\omega_0 \frac{\partial X}{\partial t} + \frac{\omega_0^2}{j\omega}\frac{\partial X}{\partial t} = -\frac{\partial^2 U}{\partial t^2} \tag{12}$$

assuming $\omega << \omega_0$, or

$$j\omega \frac{\partial X}{\partial t} + 2\lambda\omega_0 \frac{\partial X}{\partial t} + \frac{\omega_0^2}{j\omega}\frac{\partial X}{\partial t} = -j\omega\frac{\partial U}{\partial t} \tag{13}$$

assuming $\omega \cong \omega_0$, or

$$j\omega \frac{\partial X}{\partial t} + 2\lambda\omega_0 \frac{\partial X}{\partial t} + \frac{\omega_0^2}{j\omega}\frac{\partial X}{\partial t} = \omega^2 U \tag{14}$$

assuming $\omega >> \omega_0$.

The left hand side is left in terms of dX/dt because the geophone transducer responds only to velocity. Now, we find the following transfer functions:

$$\frac{\frac{\partial X}{\partial t}}{\frac{\partial^2 U}{\partial t^2}} = \frac{-j\omega}{-\omega^2 + 2j\lambda\omega_0\omega + \omega_0^2} \tag{15}$$

assuming $\omega << \omega_0$, or

$$\frac{\frac{\partial X}{\partial t}}{\frac{\partial U}{\partial t}} = \frac{\omega^2}{-\omega^2 + 2j\lambda\omega_0\omega + \omega_0^2} \tag{16}$$

assuming $\omega \cong \omega_0$, or

$$\frac{\frac{\partial X}{\partial t}}{U} = \frac{j\omega^3}{-\omega^2 + 2j\lambda\omega_0\omega + \omega_0^2} \tag{17}$$

assuming $\omega >> \omega_0$.

Generally, the natural frequency of geophones is within the band of frequencies they are intended to record. This means that the second assumption is valid and is commonly called the geophone equation. However, it should be noted that a geophone transducer should not be expected to precisely follow this equation at very low or very high frequencies. At some point it will instead follow equation (15) or (17), respectively. Equation (16) can be expressed as

$$\boxed{H_G = \frac{\frac{\partial X}{\partial t}}{\frac{\partial U}{\partial t}} = \frac{\frac{\omega^2}{\omega_0^2}}{-\frac{\omega^2}{\omega_0^2} + \frac{2j\lambda\omega}{\omega_0} + 1}}, \tag{18}$$

which is the form that will be used to generate geophone equation plots.

For an accelerometer, we modify only slightly:

$$-\omega^2 X + 2j\lambda\omega_0\omega X + \omega_0^2 X = -\frac{\partial^2 U}{\partial t^2} \tag{19}$$

assuming $\omega \ll \omega_0$, or

$$-\omega^2 X + 2j\lambda\omega_0\omega X + \omega_0^2 X = -j\omega\frac{\partial U}{\partial t} \tag{20}$$

assuming $\omega \cong \omega_0$, or

$$-\omega^2 X + 2j\lambda\omega_0\omega X + \omega_0^2 X = \omega^2 U \tag{21}$$

assuming $\omega \gg \omega_0$.

The left hand side is left as displacement output. In some MEMS accelerometers there is a system that detects displacement of a capacitor plate proof mass and acts to keep the plate centered. The signal recorded is the voltage required to keep the mass centered, which is proportional to the inhibited displacement of the proof mass. In this way it is still considered a displacement transducer. So, the three possible accelerometer transducer transfer functions are

$$\frac{X}{\frac{\partial^2 U}{\partial t^2}} = \frac{-1}{-\omega^2 + 2j\lambda\omega_0\omega + \omega_0^2} \tag{22}$$

assuming $\omega \ll \omega_0$, or

$$\frac{X}{\frac{\partial U}{\partial t}} = \frac{-j\omega}{-\omega^2 + 2j\lambda\omega_0\omega + \omega_0^2} \tag{23}$$

assuming $\omega \cong \omega_0$, or

$$\frac{X}{U} = \frac{\omega^2}{-\omega^2 + 2j\lambda\omega_0\omega + \omega_0^2} \tag{24}$$

assuming $\omega >> \omega_0$.

In MEMS accelerometers, the proof masses are very small and the silicon springs are very tight. This leads to a very high natural frequency, usually above 1 kHz. The result is that the natural frequency is much higher than the seismic band and the first assumption is valid. For this reason, equation (22) will be referred to as the accelerometer equation. It should be valid for all 'low' frequencies, but at some point the low frequency assumption will fail and the sensor transfer function will shift to equation (23). Equation (22) can be rewritten as

$$\boxed{H_A = \frac{X}{\frac{\partial^2 U}{\partial t^2}} = \frac{-\frac{1}{\omega_0^2}}{-\frac{\omega^2}{\omega_0^2} + \frac{2j\lambda\omega}{\omega_0} + 1}} \tag{25}$$

which is the form that will be used to create accelerometer equation plots. These transfer functions are consistent with those found in literature (Speller and Yu, 2001; Brincker et al., 2001; Longoria, 2000).

It may seem logical that the voltage output from an accelerometer would be the time derivative of the voltage output from a geophone, but considering both the mechanical system and the transducer system, we see that in both cases the input ground motion is modified by two time derivatives. For an accelerometer, the ground acceleration is what generates the displacement between the proof mass and the case, and then this displacement is directly transformed into the output voltage. For a geophone, the ground velocity is what generates the displacement between the proof mass and the case, and then it is the velocity of the proof mass that is transformed into the output voltage. It is the interaction between the mechanical system and the transducer system that results in differences in the amplitude and phase of some frequencies. In other words, in this case the output from the sensors is identical over a frequency range where the transfer functions have an identical response. Similarity in the transfer functions generally occurs higher in the seismic band.

When the effects of the sensor are removed, then we recover the input to the transducer. It is here that the accelerometer data is the time derivative of the geophone data. In the case of the geophone we must remove the effects of the sensor and then integrate to return to the ground motion, while for an accelerometer the sensor effects should be negligible, due to the flat amplitude and phase spectra in the acceleration domain (Maxwell, 2001), and a double time derivative will recover the ground motion.

MODELLING

The transfer functions derived above are complex, so the amplitude and phase spectra will be calculated from them as follows:

$$Amplitude = \sqrt{\mathrm{Re}(H)^2 + \mathrm{Im}(H)^2} \tag{26}$$

and

$$Phase = -\tan^{-1}\left(\frac{\mathrm{Re}(H)}{\mathrm{Im}(H)}\right) + \frac{\pi}{2} \tag{27}$$

for a geophone, or

$$Phase = \tan^{-1}\left(\frac{\mathrm{Im}(H)}{\mathrm{Re}(H)}\right) \tag{28}$$

for an accelerometer.

The phase is calculated in this way for a geophone to avoid division by zero when the input frequency equals the natural frequency. Unless otherwise stated, all plots are presented with the frequency in $\log_{10}$. Amplitudes are presented in dB and phase lag in degrees.

Some conclusions are evident simply from inspecting the derived equations. The greatest difference is that the geophone equation retains ω in the numerator while the accelerometer equation does not. The result is that as ω goes to zero, the response from the geophone transducer will also go to zero; while the result from an accelerometer transducer will go to $(1/\omega_0)^2$, the same as its response throughout the range when $\omega \ll \omega_0$. Another point is that when $\omega=\omega_0$, then the real part of both equations is zero, meaning large phase variations should be expected at the natural frequency.

As a demonstration of the different transfer functions as the ratio of the measured frequencies to the natural frequency changes, amplitude spectra for all three assumptions are shown. All of these figures are calculated for a sensor with a 10 Hz natural frequency and damping constant of 0.7. On the left are the plots assuming $\omega \ll \omega_0$, in the middle are plots assuming $\omega \cong \omega_0$ and on the right are plots assuming $\omega \gg \omega_0$. So, as transfer functions, the graphs on the left are only relevant at low frequencies, the middle graphs are relevant only near the natural frequency and the right hand graphs are relevant only at high frequencies. A global transfer function would be a hybrid of all three. Schematic versions of these figures can be found in Havskov and Alguacil (2006), along with the above equations presented as solutions for proof mass motion in terms of ground motion (no bandwidth constraints).

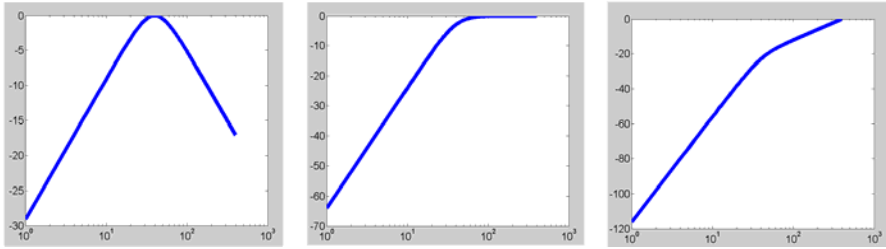

FIG. 1. Amplitude spectra with low frequency, similar frequency and high frequency assumptions for geophone.

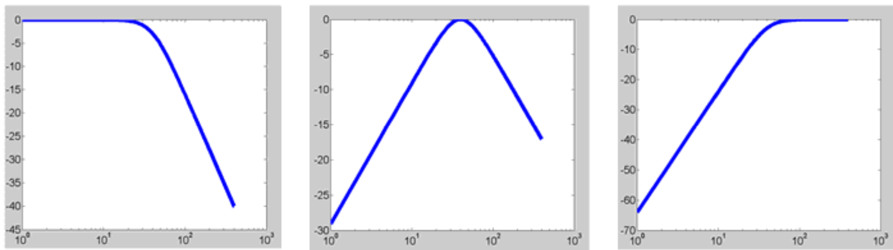

FIG. 2. Amplitude spectra with low frequency, similar frequency and high frequency assumptions for accelerometer.

A matter of interest is finding the points where one set of assumptions breaks down and the next set must be adopted. Considering these graphs as exact solutions of ground displacement (Meirovitch, 1975), velocity and displacement relative to proof mass velocity (Figure 1) or displacement (Figure 2), they can give an indication of the range of the measured frequency to natural frequency ratio over which the assumptions in the derivation of the transfer functions hold true. The damping ratio primarily controls that range.

Example transfer functions for the geophone equation (similar frequency assumption) are shown in Figures 3 through 5. Figure 3 is for values of 10 Hz resonant (natural) frequency and 0.7 damping ratio. The amplitude spectrum shows a decline from 0 dB at 20 Hz to less than -60 dB at ~0 Hz. The phase response starts around 180 degrees at ~0 Hz, descending to less than 10 degrees at 100 Hz. Stronger damping results in smoother rolloff from higher frequencies, and a slower decline in phase lag. Weaker damping (Figure 4) results in sharper rolloff, to the point where a peak around the natural frequency can be seen. This is characteristic of an underdamped system, with largest amplitudes at the natural frequency. Changing the natural frequency (Figure 5) repositions the response curves along the x axis.

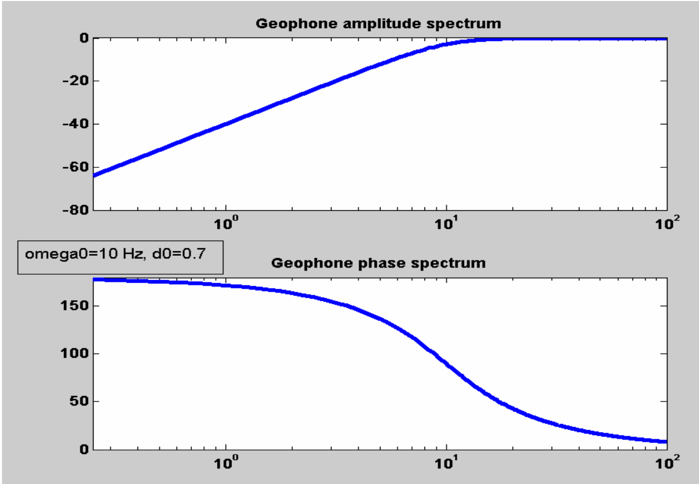

FIG. 3. Amplitude and phase spectra for a 10 Hz, 0.7 damping ratio geophone.

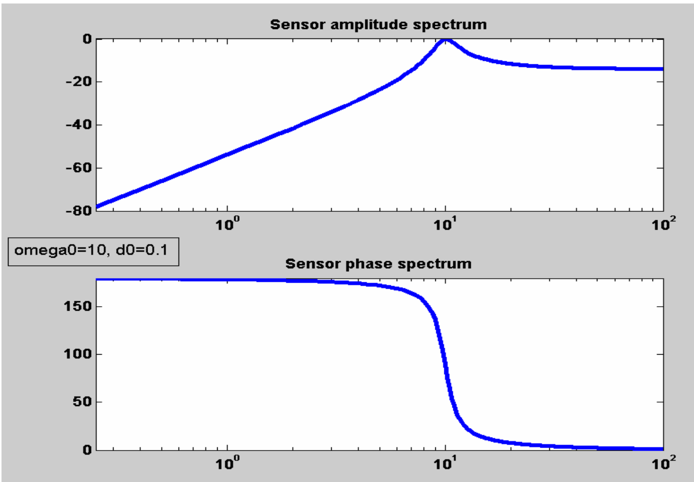

FIG. 4. Amplitude and phase spectra for a 10 Hz, 0.1 damping ratio geophone.

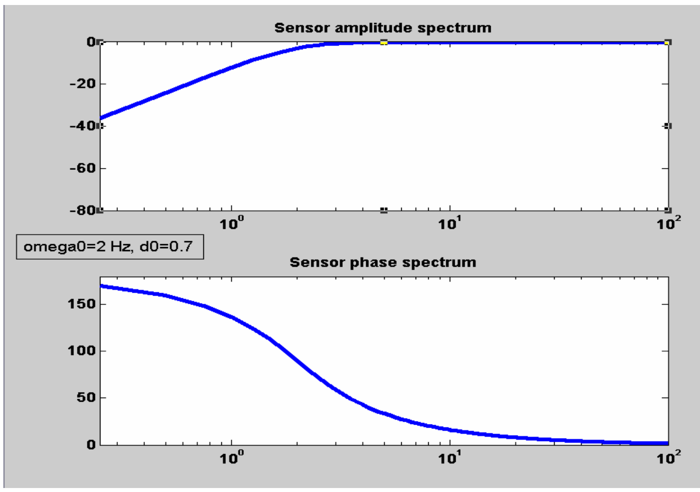

FIG. 5. Amplitude and phase spectra for a 2 Hz, 0.7 damping ratio geophone.

Another way of inspecting these results is to inverse Fourier transform the spectra to generate a transfer function wavelet. They are displayed in Figures 6 through 8, for the same parameters as Figures 3 through 5.

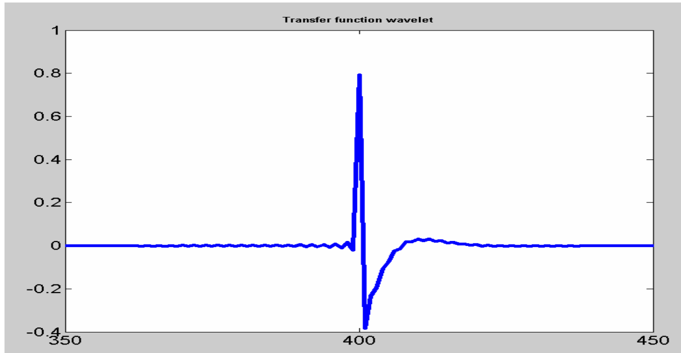

FIG. 6. Transfer function wavelet for a 10 Hz, 0.7 damping ratio geophone.

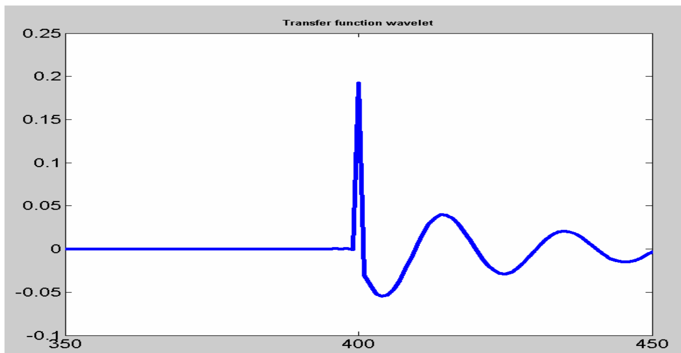

FIG. 7. Transfer function wavelet for a 10 Hz, 0.1 damping ratio geophone.

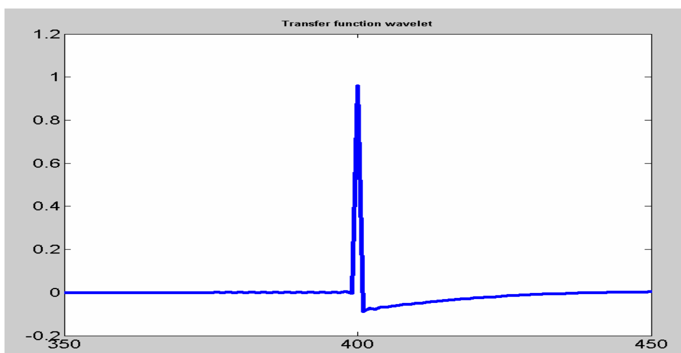

Figure 8. Transfer function wavelet for a 2 Hz, 0.7 damping ratio geophone.

When a signal is passed through the transducer, the effect is that it is convolved with the transfer function wavelet. The consequences are evident, especially in the extreme cases. Figure 7 shows that for a very under-damped sensor, the natural frequency will be amplified. Figure 8 shows that the lower natural frequency results in less transformation of the signal, since all frequencies above the natural frequency are not greatly changed (a spike would of course have no effect on an input series). Figure 6 shows that for reasonable values commonly found in modern geophones we expect the effects of the transducer to approximate a 90-degree phase shift on the transducer input. The results from passing a 1-8-60-70 Hz bandpass ground displacement wavelet (Figure 9) with the 10 Hz, 0.7 damping geophone is shown in Figure 11. Recall the transducer input is ground velocity (Figure 10).

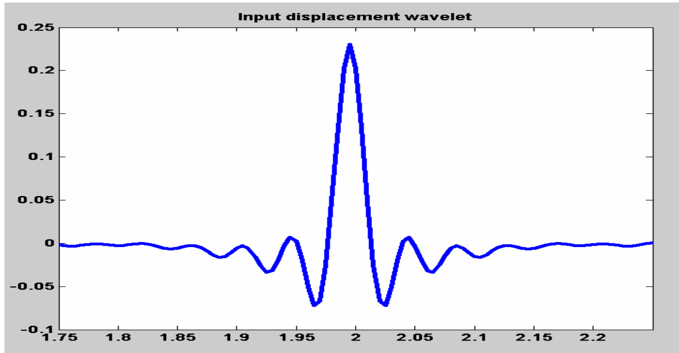

FIG. 9. Input: bandpass displacement wavelet 1-8-60-70 Hz.

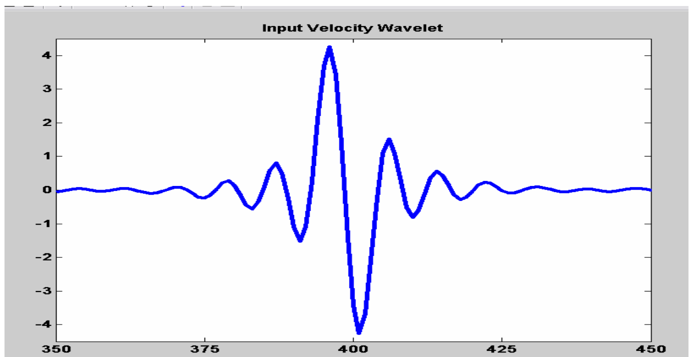

FIG. 10. Geophone input: time derivative of Figure 13.

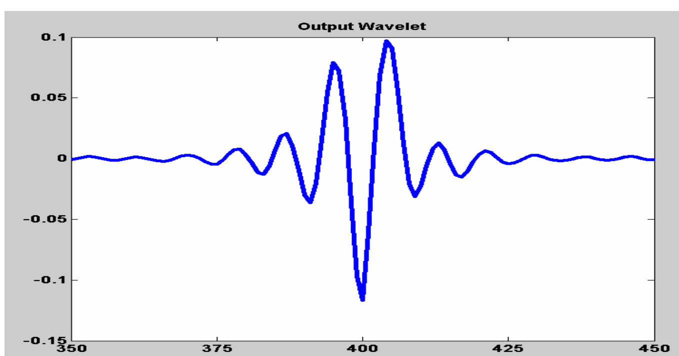

Figure 11. Output wavelet from a 10 Hz, 0.7 damping geophone.

Figure 10 shows the expected 90-degree phase shifted appearance. Figure 11 shows that in terms of the ground displacement, the output voltage is the double time derivative, with an approximate 180-degree phase shift and boosted high frequencies. The boosted high frequencies are observed by the decrease of the main peak amplitude relative to the sidelobes, and can be expected due to the fact that the double time derivative of the ground displacement is ground acceleration. These are related by

$$a = d\omega^2 , \qquad (29)$$

where a is particle acceleration, d is particle displacement and ω is angular frequency (Wikipedia, 2006).

The results for an accelerometer are far easier to predict. As long as the assumption that the measured frequencies are low compared to the natural frequency, the response in both amplitude and phase will be zero. The analysis presented here is bandlimited to 100 Hz, and this will result in the accelerometer transfer function wavelet being wider than a spike. Changing the natural frequency of the accelerometer until deviations from zero are observed is simply invalidating the assumption that went into the derivation. There was no assumption concerning damping ratio, however, so its effects on a 1000 Hz accelerometer will be investigated in Figures 12 and 13.

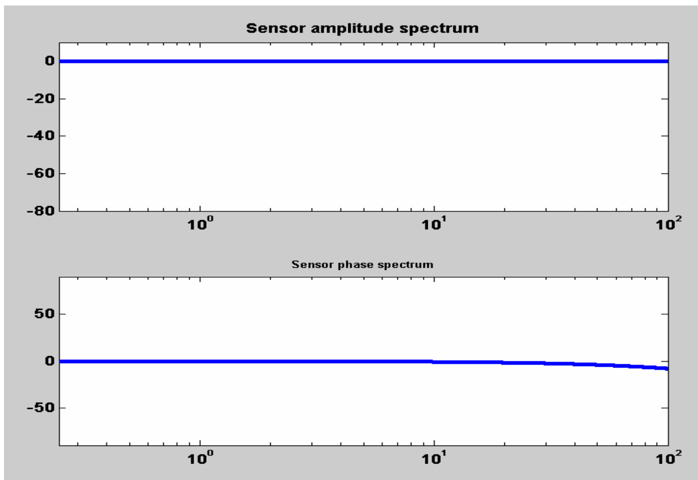

FIG. 12. Amplitude and phase spectra of a 1000 Hz, 0.7 damping ratio accelerometer.

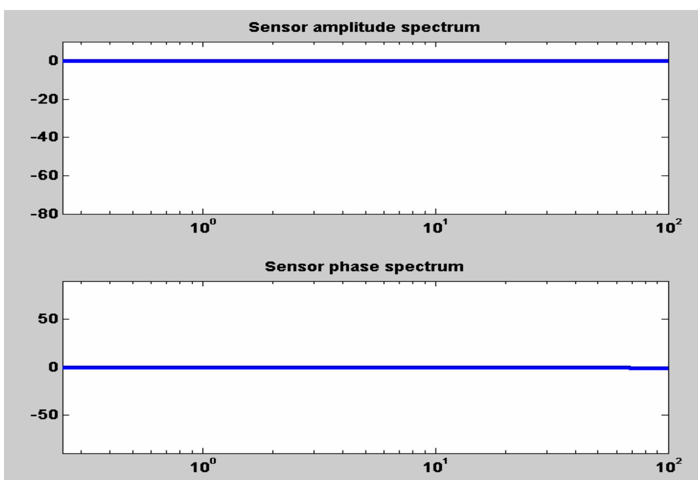

FIG. 13. Amplitude and phase spectra of a 1000 Hz, 0.1 damping ratio accelerometer.

Figure 12 shows a damping ratio of 0.7. It is possible to see that the phase deviates slightly from zero near 100 Hz. With a lower damping ratio of 0.1 (Figure 13), the deviation is barely perceptible, showing that a lowered damping ratio extends the range of the linear phase response. However, only frequencies up to 100 Hz are shown, and significant amplitude effects would be introduced just above 100 Hz at such a low damping ratio. Generally it can be said that damping near 0.7 extends the linear range of the amplitude spectrum, while introducing changes to the phase spectrum sooner than a lower ratio. Figures 14 and 15 show the transfer function wavelets for these two cases, and Figure 17 shows the output wavelet after convolution with the acceleration-domain bandpass 1-8-60-70 wavelet (Figure 16).

Figures 14 and 15 show the expected bandlimited peak for the transfer function wavelet. Some phase effects at high frequencies, introduced by the high damping ratio, are evident in Figure 15, and subdued in Figure 16. The output wavelet (Figure 18) is similar to the output from the geophone, but without the phase and amplitude effects at low frequencies.

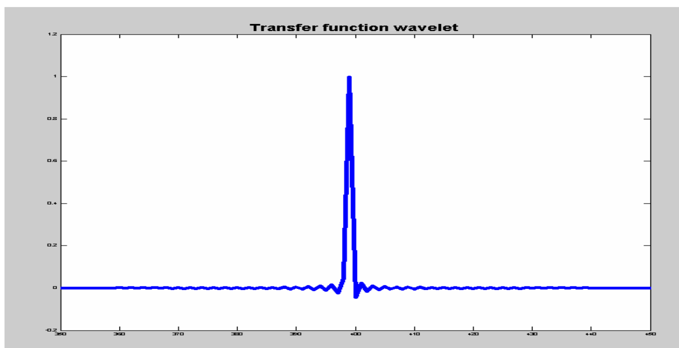

FIG. 14. Transfer function wavelet of a 1000 Hz, 0.7 damping ratio accelerometer.

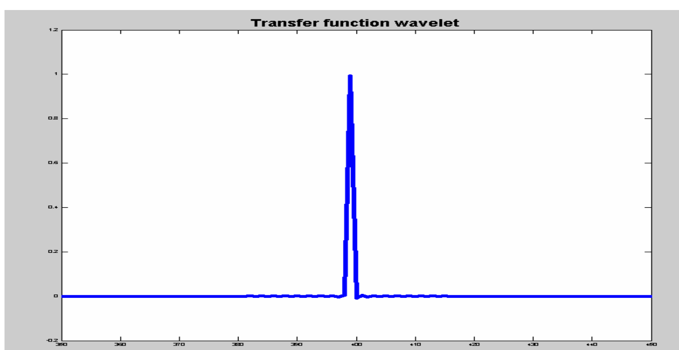

FIG. 15. Transfer function wavelet of a 1000 Hz, 0.1 damping ratio accelerometer.

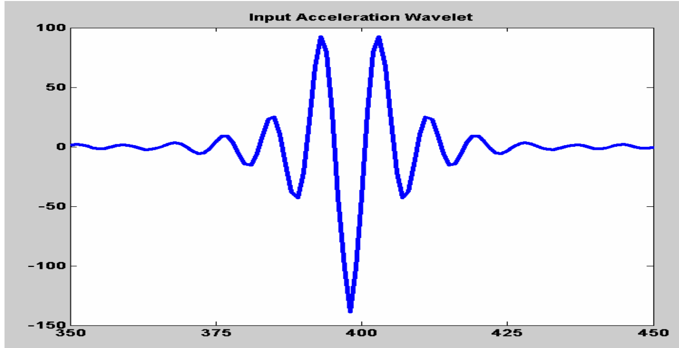

FIG. 16. Accelerometer input: double time-derivative of Figure 13.

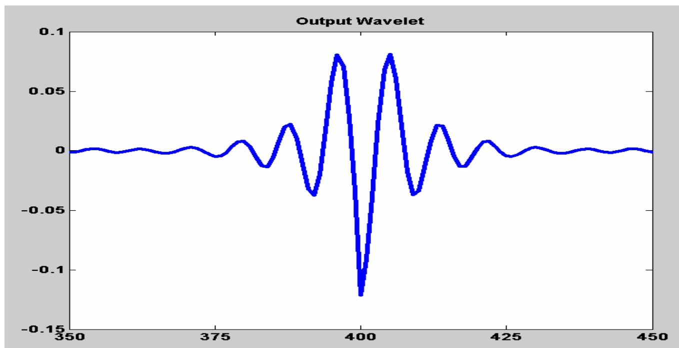

FIG. 17. Output wavelet from a 1000 Hz, 0.7 damping ratio accelerometer.

When all frequencies arriving at the sensor have been recorded according to the specifications of the geophone manufacturer, then any changes to the waveform can be removed easily by deconvolving with the manufacturer's amplitude and phase spectra. If any significant deviation from the manufacturer's specifications has occurred, then the input waveform would not be precisely recovered. This is where the flat amplitude and phase spectra of an accelerometer would be of most value. Since the geophone equation is not derived for recording very low frequencies relative to the natural frequency, it should not be expected to be accurate where that is true.

CONCLUSIONS

Transfer functions for geophone and accelerometer transducers are derived and modeled. These equations are true over all frequencies when relating ground motion to proof mass motion, but are only transfer functions when they represent transducer output divided by transducer input. Lower natural frequencies appear beneficial for geophones while higher natural frequencies are better for accelerometers. Damping ratio around 0.7 extends the range of frequencies free of amplitude effects, but narrows the range free of phase effects. The transfer functions are inspected graphically using amplitude and phase spectra and transfer function wavelets derived from them. Convolution of an input wavelet with the transfer function spectra shows that voltage output from both a geophone and an accelerometer is similar to a double time-derivative of the ground displacement.

ACKNOWLEDGEMENTS

Thanks to the CREWES sponsors for their support.

REFERENCES

Text

Brincker, R., Lago, T. L., Andersen, P. and Ventura, C.; 2001; Improving the classic geophone element by digital correction; In Proceedings of the 23rd International Modal Analysis Conference; **38**; 2; 131-140

Havskov, J and Alguacil, G; 2006; Instrumentation in Earthquake Seismology, 1st edition; Springer; p. 25-27

Longoria, R. F.; 2000; Dynamic Systems and Controls Lab Notes; Department of Mechanical Engineering, University of Texas (Austin)

Lowrie, W.; 1997; Fundamentals of Geophysics; Cambridge University Press; p. 104-108

Maxwell, P.; 2001; Sensor improves image quality; Hart's E&P; Sept.; 41-42

Meirovitch, L; 1975; Elements of Vibration Analysis; McGraw-Hill; p. 52-55

Speller, K. E. and Yu, D.; 2004; A low-noise MEMS accelerometer for unattended ground sensor applications; SPIE Defense and Security Symposium Proceedings; Society of Photo-Optical Instrumentation Engineers

Internet

Atis telecom glossary: http://www.atis.org/tg2k/_transfer_function.html

Keller, F.; 2006; Seismometer Documentation; TU Clausthal; http://www.ifg.tu-clausthal.de/java/seis/seis_doc-e.html

Wikipedia authors; 2006; Particle displacement; Wikipedia; http://en.wikipedia.org/w/index.php?title=Particle_displacement&oldid=82695519

APPENDIX A

The following equations (A1-A9) and the accompanying derivation can be found in Lowrie (1997). For descriptions of what is occurring within the sensor we rely on Keller (2006). Sensors for seismic exploration are generally an inertial mass (M) suspended by a spring from a frame, which is coupled to the earth. When the earth is displaced by a seismic wave, the frame displaces relative to the inertial mass. The amount the frame moves relative to the proof mass (i.e., the amount of stretch in the spring), is x. This is the displacement detected by the transducer, which will transform it into the electrical output. If there is no motion of the proof mass relative to the frame, there is nothing for the sensor to detect.

The ground displacement is u. Note that whenever the ground motion is upwards, the deflection of the proof mass relative to the frame will be downward, and vice versa. The net motion (i.e., the movement of the proof mass when viewed from outside) is n, which is equal to x+u. This is illustrated in Figure A1.

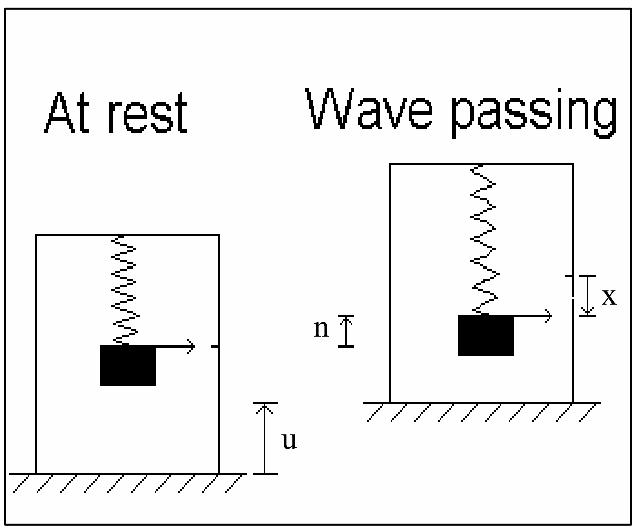

Figure A1. Proof mass motion as a wave passes. Ground motion is u, proof mass motion relative to the frame is x, and the net motion is n.

The equation of motion for the sensor system is then

$$M \frac{\partial^2}{\partial t^2}(x+u) = -kx . \tag{A1}$$

This can also be described as balancing external forces (left-hand side) and internal forces (right-hand side) acting on the proof mass (Keller, 2006). Defining $k=(\omega_0)^2M$, where ω_0 is the natural frequency, gives the equation for simple harmonic motion:

$$\frac{\partial^2 x}{\partial t^2} + \omega_0^2 x = -\frac{\partial^2 u}{\partial t^2}. \tag{A2}$$

However, a sensor defined by this equation is undamped and would be overcome by ground motions near its natural frequency, rendering it unable to record any other frequencies. For this reason seismic sensors are damped by a force proportional to the velocity of the frame relative to the inertial mass. This damping is expressed as a new term in the equation of motion for the sensor:

$$\frac{\partial^2 x}{\partial t^2} + 2\lambda\omega_0 \frac{\partial x}{\partial t} + \omega_0^2 x = -\frac{\partial^2 u}{\partial t^2}, \tag{A3}$$

where λ is the damping ratio.

Looking now at the simplest possible case, we assume ground motion $u=A\cos(\omega t)$. With critical damping ratio ($\lambda=1$), a solution for the displacement of the proof mass relative to the sensor frame is given by

$$x = \frac{A\omega^2}{\omega_0^2 + \omega^2}\cos(\omega t - \Delta), \tag{A4}$$

where

$$\Delta = \tan^{-1}\left(\frac{2\omega\omega_0}{\omega_0^2 - \omega^2}\right). \tag{A5}$$

Zero displacement ($x=0$) is defined as where the proof mass hangs when the sensor is at rest.

Three cases can be seen as the ratio between ω and ω_0 changes. In designs where the natural frequency of the system is much lower than the driving frequency band, then $\omega >> \omega_0$ and the simplified equation becomes

$$x \cong A\cos(\omega t) = u, \tag{A6}$$

and

$$\Delta \cong 0. \tag{A7}$$

In this simplified case, the displacement of the proof mass relative to the sensor frame is proportional to ground displacement. Mechanically, when frequencies are very high compared to resonance, the proof mass does not move much at all. This is because the spring is very loose and before it can pull the mass one way, the frame has already moved the other way. Since the mass stays stationary when viewed from outside the sensor, the displacement of the frame relative to the mass is similar to the displacement of the ground relative to its initial position. Thus we can say that when the recorded frequencies are much higher than the natural frequency the sensor responds to ground displacement.

If the natural frequency is much higher than the recorded frequency band, we can say $\omega \ll \omega_0$, and the simplified equation becomes

$$x \cong \frac{\omega^2}{\omega_0^2} A\cos(\omega t) = -\frac{1}{\omega_0^2}\frac{\partial^2 u}{\partial t^2}, \tag{A8}$$

and again

$$\Delta \cong 0. \tag{A9}$$

This shows the displacement of the proof mass relative to the sensor frame is proportional to ground acceleration. Mechanically, when frequencies are very low compared to resonance, the motion of the proof mass closely follows the motion of the frame, so relative displacement is near zero. This is because the spring is very tight and it is only upon acceleration of the frame (due to acceleration of the ground) that any relative displacement occurs. This means that when the natural frequency is well above the recorded frequency band then the sensor responds to ground acceleration.

In the case where ω and ω_0 are similar, the displacement of the proof mass relative to the sensor frame is proportional to the velocity of the ground. This is because the spring is neither very loose nor very tight. As the velocity of the sensor frame increases, the spring is strong enough to pull the proof mass along with it, but not strong enough to return the proof mass to its initial position relative to the frame. As long as the frame travels with some velocity, the displacement of the proof mass relative to the frame stays about the same. If the velocity increases then the displacement increases, and if the velocity returns to zero then the proof mass returns smoothly to its initial position, under the influence of damping. This means that when the natural and recorded frequencies are similar (i.e., in between the extreme cases), then the sensor responds to ground velocity.

As shown above, the mechanical output depends on the ratio of its natural frequency to the measured frequencies, which is dependent on its design. This is one consideration when deriving a transfer function for a transducer. The other consideration is how the transducer converts the input motion to an electrical signal (Keller, 2006). Technically, all transfer functions derived in this paper are for the transducer: that is, they are found by dividing the transducer output by the transducer input. The transducer input is the mechanical output.

There are generally two types of transducers used in seismic sensors: displacement and velocity. MEMS sensors use displacement transducers, generally in the form of capacitance bridges that measure the change in capacitance as the distance between capacitor plates changes. Piezoelectric crystals can also be used to detect displacement changes. Geophones, on the other hand, use magnetic induction, which does not respond to displacement. Magnetic induction occurs only when flux changes, and when in the presence of a permanent magnet, this requires velocity between the measurement circuit and the magnet.